Transworld Research Network
37/661 (2), Fort P.O., Trivandrum-695 023, Kerala, India

Recent Res. Devel. Physics, 5(2004): 141-158 ISBN: 81-7895-126-6

6

Doping the ferromagnetic high-T_c superconductor $RuSr_2RECu_2O_8$ (RE=Gd, Eu)

A. Hassen[1], A. Krimmel[1], J. Hemberger[1], A. Loidl[1] and P. Mandal[2]
[1]Institut für Physik, Elektronische Korrelationen und Magnetismus, Universität Augsburg D-86159 Augsburg, Germany; [2]Saha Institute of Nuclear Physics, 1/AF Bidhannagar Calcutta, 7000064, India

Abstract

Doping experiments on the ferromagnetic superconductor $RuSr_2RECu_2O_8$(RE=Gd,Eu) are reviewed. Single phase polycrystalline samples were synthesized by conventional solid-state reactions and different methods of sample preparation are discussed. Within the studied levels of different cation substitution no significant structural changes could be observed. A summary of various doping experiments at the Ru site is given. The transport properties of La-doped Ru-1212RE are investigated in detail. With increasing x, the superconducting transition T_c becomes rapidly suppressed. The substitution at the copper site by A = Ga, Co, Ni, Mn and Zn in $RuSr_2RE(Cu_{1-x}A_x)_2O_8$ compounds is studied and compared to previous results, as well as to other high-T_c superconductors. Independent of the type of A cations (for doping levels up to 3%), the magnetic ordering temperature T_M does not change while superconductivity is strongly suppressed.

Correspondence/Reprint request: Dr. A. Krimmel, Institut für Physik, Elektronische Korrelationen und Magnetismus, Universität Augsburg, D-86159 Augsburg, Germany. E-mail: alexander.krimmel@physik.uni-augsburg.de

1. Introduction

The antagonistic nature of superconductivity and ferromagnetism was studied theoretically by Ginzburg [1] in 1956, while experimental progress in the field began after the discovery of the so-called Chevrel phases $REMo_6X_8$ (RE=rare earth, X=S, Se) or in $RERh_4B_4$ (see for example Ref. [2]). In many of these compounds, superconductivity with a critical temperature T_c coexists with antiferromagnetic (AFM) order below the Néel temperature T_N where $T_N \ll T_c$. On the other hand, singlet superconductivity and ferromagnetism can not coexist in bulk samples with realistic physical parameters. However, under certain conditions the ferromagnetic order is transformed, in the presence of superconductivity, into a spiral or domain-like structure depending on the type and strength of magnetic anisotropy in the system [3]. The internal field of a ferromagnetically ordered state leads to a Zeeman splitting of the Fermi surface that excludes electron pairing of opposite spin and momentum. Allowing for finite angular momentum of electron pairs led to the theory of Fulde-Ferrel-Larkin-Ovchinnikov (FFLO) superconductivity [4], where a suitable spatial modulation of the superconducting or ferromagnetic order parameter (or both) leads to their mutual coexistence.

Recently, a new class of magnetic superconductors among the layered perovskite ruthenocuprates $RuSr_2RECu_2O_8$ (Ru-1212RE, RE = Gd, Eu, Y and Sm) has been synthesized [5]. In particular, the Ru-1212Gd system has attracted great interest since it exhibits a ferromagnetic transition at $T_M \approx 135$ K and bulk superconductivity below $T_c \approx 46$ K, depending on the sample preparation conditions [6–8]. For the isostructural Ru-1212Eu compound, these transitions are shifted to approximately 133 K and 32 K, respectively. Therefore, these compounds represent model systems for studying the interplay between superconductivity and ferromagnetism.

Neutron powder diffraction measurements on Ru-1212RE [9, 10] revealed a *G*-type AFM structure of the Ru sublattice with an ordered magnetic moment of the order of $1\mu_B$. The Gd ions order independently below 2.5 K also in a *G*-type spin configuration. Both diffraction studies put an upper limit of 0.3 μ_B [9] or 0.1 μ_B [10] to any net zero-field ferromagnetic (FM) moment. Later on, from low-field magnetization measurements on Ru-1212Eu it has been concluded that the FM moment is of the order of 0.05 μ_B/Ru at 5 K [11]. The origin of the FM moment is still unclear. Weak ferromagnetism can have its origin in the Dzyaloshinski-Moriya interaction. There is an ongoing dispute if the symmetry of the Ru-1212RE compounds allows for a non-zero antisymmetric superexchange [10]. Another source of providing a canting of the Ru spins would be the double-exchange interaction which is responsible for the occurrence of ferromagnetism in the manganites [12]. The mixed valent state of the Ru ions, as evidenced by XANES [13] could enable such a double exchange. And indeed, recently the double-exchange mechanism has been proposed to be responsible for the weak ferromagnetism in the rutheno-cuprates [14]. Finally, based on detailed NMR studies [15] the possibility of ferrimagnetism in a charge-ordered state of the RuO_2 planes has been suggested.

The proportion of Ru^{4+} /Ru^{5+} ions may be changed by cation substitution in Ru-1212RE. Therefore, the hole concentration in the superconducting CuO_2 planes may be modified in a controlled way by doping [13]. In case of the cuprate superconductors, hole carriers can be induced either by cation substitution (as in $La_{2x-1}Sr_xCuO_4$) or by

oxygen intercalation (as in $YBa_2Cu_3O_{7-\delta}$) or by a combination of them. Unlike the cuprates, the oxygen content of Ru-1212RE can virtually not be changed. Thermogravimetric experiments [16, 17], as well as the thermoelectric power (TEP) [18] indicate that the oxygen content is always very close to 8. In order to change the hole carrier concentration in Ru-1212RE, one therefore has to rely on cation substitution [19, 20] which represents one essential motivation for doping experiments.

In this work, we first give a detailed account on the sample preparation. Next we present various doping experiments of Ru-1212RE at the Ru and Sr site respectively and discuss the previously established generalized phase diagram of the Ru1212 system. Moreover, we show the difference between La-doped Ru-1212Gd and Ru-1212Eu. Finally, the effect of different magnetic and nonmagnetic cations at the copper site is studied and compared to previous results on Ru-1212RE, as well as to other high-T_c superconductors. The results are summarized in the final conclusion section.

2. Sample preparation and experimental techniques

2.1. Sample preparation

One problem of synthesizing Ru-1212RE compounds is the formation of some stable impurity phases during the chemical reactions. These impurities are attributed to $SrRuO_3$ [5] or Gd_2CuO_4 [21] which show magnetic order below 165 and 265 K, respectively. Otzschi *et al.* [16] reported that once $SrRuO_3$ is formed during the sample preparation, it does not decompose or disappear completely even after sintering the sample at high temperature due to its chemical stability. The occurrence of parasitic phases and the superconducting and magnetic properties of these compounds depend sensitively on the details of the sample preparation procedures. Therefore, the reaction atmosphere and the calcination temperature and time must be optimized.

Polycrystalline samples of pure Ru-1212RE (RE=Gd, Eu) have been synthesized by a solid-state reaction method [5]. High purity RuO_2, $SrCO_3$, Gd_2O_3, Eu_2O_3 and CuO powders were selected. Both Gd_2O_3 and Eu_2O_3 are dried at 1000 °C for 15 h. All the following steps are important to minimize any impurity phases. The powders were mixed in an appropriate ratio and calcined at 930 °C in air. The product was ground, pressed into pellets and heated at 1020 °C in nitrogen atmosphere for 12 h. The pellets were reground into fine powders and put into a furnace again at 1040 °C for 12h in oxygen, followed by slow cooling. The sintering was repeated twice at 1050 and 1055 °C with intermediate grindings. Finally the samples were again pressed into pellets and annealed for 6 days at 1060 °C in oxygen and cooled slowly at a rate of 30 °C/h to room temperature. For Ru-1212Eu samples the sintering temperatures are slightly lower than that for Ru-1212Gd samples by 10 °C. Some samples of Ru-1212Gd were annealed for further 6 days (thus 12 days in total) under the same conditions to study the effect of long-term annealing on the superconducting and magnetic properties. Fig. 1 shows the dc-resistivity of two Ru-1212Gd samples tempered for 6 or 12 days, respectively. From Fig. 1, it is evident that the resistivity of the further annealed sample is below that of ceramics annealed for 6 days (as-prepared). The zero resistance temperature $T_c(R = 0)$ is shifted to a slightly higher temperature while the onset temperatures of superconductivity, as well as T_M, do not change for both samples. The difference between the as-prepared and the further annealed samples can also be observed by studying the field dependence of the resistivity at constant temperature ($T = 20$ K), as

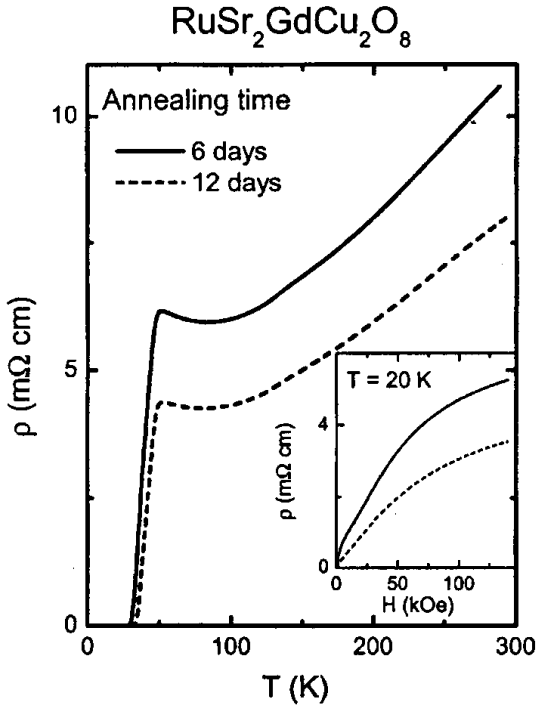

Figure 1. Dc resistivity versus temperature of Ru-1212Gd for two different samples annealed for either 6 days (solid line) and 12 days (dashed line), respectively. The inset illustrates the difference between the two samples by showing the field dependent resistivity at 20 K.

shown in the inset of Fig. 1. With increasing magnetic fields the resistivity of both samples increases. Analogous to the temperature dependence, the field dependent resistivity is smaller for the further annealed than for the as-prepared sample. A similar behavior was observed by Tallon *et al.* [22] studying two different Ru-1212Gd samples, one virgin (not annealed) and the other annealed for 6 days.

One interpretation of these results was that heat treatment affects the conductivity related to the grain boundaries [16, 23] or, alternatively, that longer temper times may increase the hole carrier concentration [22]. Moreover, Artini *et al.* [7] demonstrated that for annealing at high temperatures $T > 1170$ °C, there is a tendency to introduce disorder in the system and a subsequent decrease of the transition temperature is observed. This emphasizes again the importance of sintering time and temperature on the superconducting properties of these compounds.

Pure Ru-1212RE samples can also be prepared in a two-step procedure [5,24]. First, the precursor Sr_2RERuO_6 (Sr-2116) is prepared from stoichiometric quantities of RuO_2, RE_2O_3 and $SrCO_3$. The mixed powders were ground and calcined at 950 °C in air. The products were reground, pressed into pellets and fired at 1250 °C in air. In the second step, the obtained Sr-2116 precursor phase was mixed with CuO and the mixture was ground, milled, pressed and fired for 5 days at 1060 °C in oxygen.

After optimizing the sample preparation method for the pure compounds, doped samples were synthesized by the same techniques (solid state reaction) and identical annealing conditions. In addition to the chemical powder components of pure Ru-1212RE, high purity La_2O_3 powders are used to prepare $Ru(Sr_{1-x}La_x)_2RECu_2O_8$

compounds with $0 \leq x \leq 0.10$. Additional appropriate quantities of high purity powders of ZnO, NiO, CoO, MnO and Ga_2O_3 are used to prepare $RuSr_2Gd(Cu_{1-x}A_x)_2O_8$, where A = Zn, Ni, Co, Mn and Ga with $0 \leq x \leq 0.03$. For other doped compounds such as $RuSrGd_{1-x}Ce_xCu_2O_8$ [25] or $Ru_{1-x}M_xSr_2GdCu_2O_8$ (M = Ti and Rh) [26], it was found that instead of nitrogen, an argon atmosphere is more suitable to minimize the impurity phases.

2.2. Experimental techniques

2.2.1. X-ray diffraction

All samples were characterized by powder x-ray diffraction (PXD) at room temperature on a Stoe x-ray diffractometer using Cu-K_α radiation (λ = 1.5406 Å) in an angular range of $20^o \leq 2\theta \leq 80^o$ at an increment of 0.02^o. The data were analyzed by standard Rietveld refinement employing the FULLPROF program [27].

2.2.2. Magnetic measurements

Magnetic DC-susceptibility (defined as $H_{dc} = M/H$) measurements were performed using a commercially available SQUID magnetometer (Quantum Designs, MPMS) in the temperature range $2 \leq T \leq 400$ K at two different fields of H_{dc} = 0.5 and 5 Oe, respectively. Additionally, an induction bridge has been employed for AC-susceptometry and field dependent DC-extraction magnetization measurements in an Oxford cryo-magnet in fields up to 140 kOe and in the temperature range $1.5 \leq T \leq 300$ K. The AC-susceptibility has been recorded at different frequencies (1 Hz $\leq \nu \leq$ 1 kHz) for a constant driving field of H_{ac} = 0.1 Oe_{rms} or, alternatively, at a constant frequency (ν= 1 Hz or 1 kHz, respectively) for different driving fields 0.1 $Oe_{rms} \leq H_{ac} \leq 10$ Oe_{rms}.

2.2.3. Electrical resistivity

The electrical transport investigations have been carried out in the same Oxford cryo-magnet. DC-resistance and magnetoresistance was measured by a conventional four-probe technique in the temperature range $2 \leq T \leq 300$ K.

2.2.4. Thermoelectric powder

The thermoelectric power S of various Ru-1212 compounds was measured in the temperature range $77 \leq T \leq 300$ K by a differential technique. A temperature gradient is created between the two ends of a sample and the corresponding voltage evolving between the hot and cold end is recorded. The temperature difference was kept fixed at (approximately) 0.5 K during a complete temperature sweep [28].

3. Crystal structure

The crystallographic structure of Ru-1212RE is shown in Fig. 2. It is closely related to that of the prototype high-T_c cuprate superconductor $YBa_2Cu_3O_{7-\delta}$ (YBCO) [6, 20, 29]. The main difference is that the Cu-O chains of YBCO are replaced by square planar Ru-O layers in Ru-1212RE. Gd, Sr and Ru substitute Y, Ba and Cu (of the Cu-O chains), respectively. Ru is sixfold coordinated by oxygen atoms, forming RuO_6 octahedra, while Cu is five-fold coordinated by O, resulting in CuO_5 square pyramids. Neutron diffraction [29] showed that the interatomic distance between Cu and its apical oxygen is

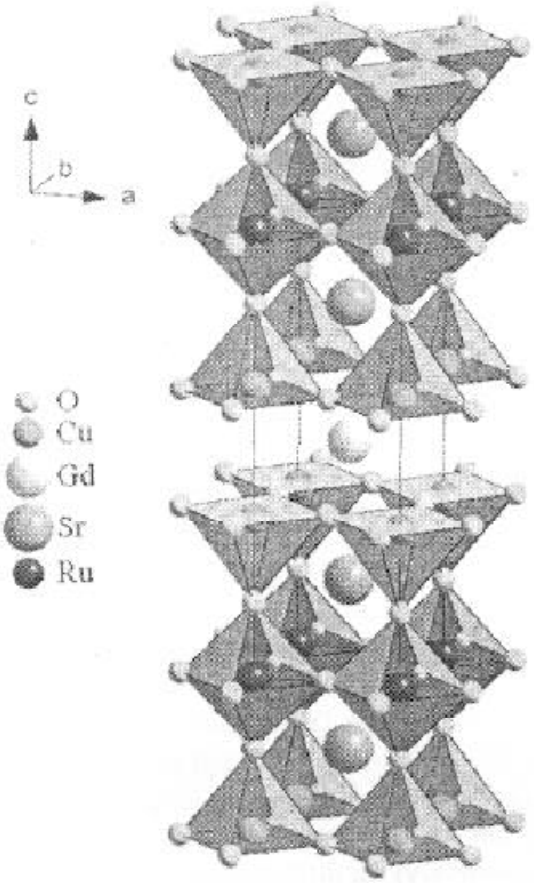

Figure 2. The crystal structure of $RuSr_2GdCu_2O_8$ with the Cu atoms located at the center of the base of the square pyramids and the Ru atoms at the center of the octahedra.

significantly larger (2.19 Å) than that of Ru and its corresponding apical oxygen ion (1.912 Å). This may yield to an essentially two-dimensional (2D) electronic structure of the CuO_2 layers [30].

The crystal structure of Ru-1212RE is tetragonal with space group *P4/mmm* and lattice parameters a = 3.836 Å and c = 11.56 Å [6, 20, 29, 31]. Studies of the microstructure of Ru-1212RE by high resolution x-ray [32] and neutron [29] powder diffraction, as well as by electron microscopy [32, 33] revealed two types of superstructures. One due to tilting of the RuO_6 octahedra around the c–axis and a second due to vacancy ordering along the b–axis. The bond angle ϕ of Cu-O-Ru strongly affects the transport and magnetic properties of this system [26, 34]. It should be noticed that a clear correlation between crystal structure and the appearance of superconductivity could not be established yet. In some cases the samples remain non-superconducting though they exhibit the same symmetry and crystal metric [6].

All investigated compounds presented here show tetragonal symmetry described by space group *P4/mmm*. For pure Ru-1212RE the Ru atoms are located at the Wyckoff position (1*b*)(0, 0, 1/2), RE at the (1*c*) site (1/2, 1/2, 0), Sr occupies the 2*h* position (1/2, 1/2, *z*), Cu is found at (2*g*) (0, 0, *z*), whereas the oxygen ions are distributed among the (8*s*) (x, 0, *z*), (4*i*) (0, 1/2, *z*) and (4*o*) (*x*, 1/2, 1/2) positions, respectively. Within the

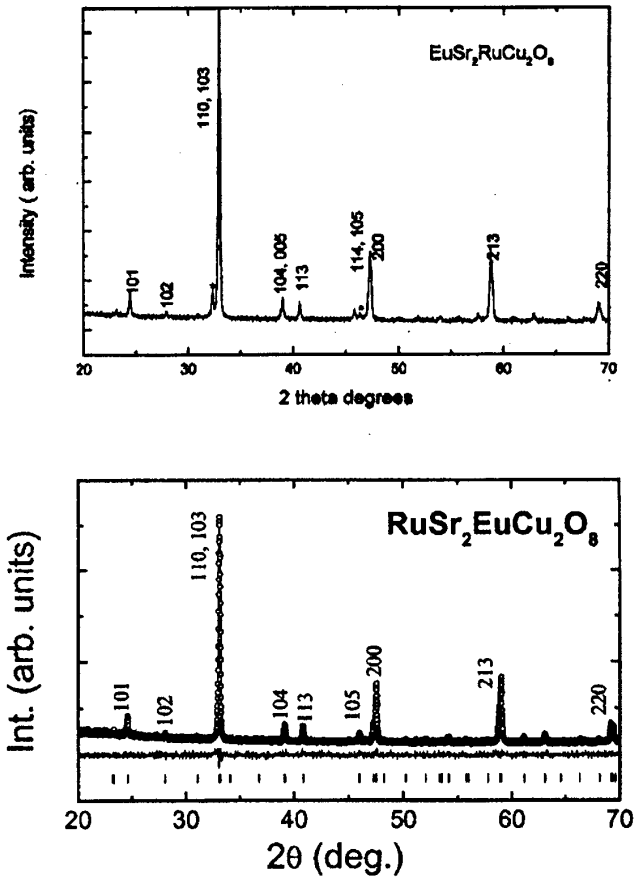

Figure 3. X-ray diffraction patterns of $RuSr_2EuCu_2O_8$. The upper frame shows data from the literature [6] and the lower frame one of our samples. The vertical bars at the bottom of the diagrams (lower frame) denote the calculated peak positions. Open circles and full line correspond to measured and calculated intensities, respectively.

studied concentration range of doping, no significant change of the crystal structure could be observed.

Based on the Rietveld analyses of x-ray diffraction patterns, all samples are found to be single phase except for the pure Eu-based compounds which exhibit an additional very weak intensity close to $2\theta \approx 32^o$. This spurious reflection is usually attributed to residues of $SrRuO_3$ or Gd_2CuO_4 [21] and its occurrence is well-known for the Ru-1212RE system. Exemplarily, Fig. 3 shows the x-ray diffraction patterns of pure Ru-1212Eu after having optimized the sample preparation procedures (lower frame) and compares it with data from the literature [6] (upper frame). Some weak additional intensities are observed close to $2\theta \approx 32^o$ or $2\theta \approx 46^o$ (see upper frame of Fig. 3). Based on the x-ray diffraction data alone it is not possible to identify these spurious phases. It becomes clear that the amount of parasitic phases is minimized in our samples. Moreover, no anomalies in the magnetic measurements close to the magnetic ordering temperatures of $SrRuO_3$ (T_c = 165 K) or Gd_2CuO_4 (T_N = 265 K) could be observed, corroborating that the amount of spurious phases in our samples is marginal.

4. Doping at the Ru site: Ti, Rh, Nb, V, Cu

The effect of substituting cations on the physical properties of Ru-1212Gd was investigated by different groups [13, 20, 25, 26, 34–37]. Both magnetism and superconductivity strongly depend on the type of dopant and the substitutional site. Focusing first on substitutional series at the Ru site, McLaughlin and Attfield [20] investigated $Ru_{1-x}Sn_xSr_2GdCu_2O_8$. They observed that Sn defects suppress the FM moment in the Ru layers and the magnetic ordering temperature (T_m) decreases from 138 K in the pure compound to 78 K for $x = 0.4$. On the other hand, the superconducting transition temperature (T_c) is increased from 36 K in the undoped material ($x = 0$) to 42 K for $x = 0.2$. These results were attributed to the diamagnetic properties of the Sn ions that do not contribute to the magnetic properties and therefore the total magnetic moment in the RuO_2 layers is reduced. Furthermore, the enhancement of the superconducting transition temperature in Sn-doped compounds may also reflect an increase of the charge carrier density in the copper planes. This result is different from observations in Nb-doped compounds [20] in which the substitution of Ru by Nb^{5+} decreases both T_M and T_c. Also the variation of the room-temperature Seebeck coefficient on Nb or Sn doping is different. Most probably the number of holes is increased for Sn, but decreased for Nb doping. Similarly, the magnetic and superconducting properties of $Ru_{1-x}M_xSr_2GdCu_2O_8$, with M = Ti, V and Nb for $x = 0.10$ and 0.20, have been investigated by Rijssenbeek *et al.* [36] and Malo *et al.* [37]. Both T_c and T_M were found to decrease for T_i and Nb, but are enhanced for V at low doping levels. However, superconductivity becomes fully suppressed for all samples at higher concentrations.

The substitution of Ru by non-isoelectronic defects additionally changes the charge reservoir. Substituting Ti^{4+} ($3d^0$) and Rh^{3+} ($4d^6$) for Ru reduces the onset of ferromagnetism and superconductivity, but at a different rate. In the Ti-doped compounds, the corresponding magnetic and superconducting transition temperatures T_M and T_c decrease significantly faster than in Rh-doped samples. Superconductivity becomes fully suppressed at $x = 0.1$ for Ti and $x = 0.2$ for Rh, respectively [26]. These results are consistent with experiments on Nb-doped compounds [20]. Despite the fact that the hole concentration is increased, the superconducting transition temperature decreases for both dopants, most probably due to disorder that prevents charge delocalization between adjacent RuO_2 and CuO_2 layers [26].

Dilution of the magnetic Ru sublattice was studied in the substitutional series $Ru_{1-x}Sr_2GdCu_{2+x}O_8$ [35]. Substituting Cu for Ru corresponds to an increased hole doping and in that case a clear correlation between Cu concentration and superconducting transition temperature could be established. Starting from pure Ru-1212Gd with $T_c = 45$ K the onset temperature of superconductivity steeply raises upon Cu doping, reaching values of $T_c = 72$ K for $x = 0.3$ and 0.4 before decreasing again for still higher Cu concentrations. For $x > 0.1$ no irreversibility of the magnetization in the normal state could be observed anymore, indicating the absence of long range weak ferromagnetic order in the Cu doped compounds [35].

5. Electron and hole doping at the Sr site: La, Na

Fig. 4 shows the temperature dependent resistivity $\rho(T)$ of $Ru(Sr_{1-x}La_x)_2RECu_2O_8$, where RE = Gd (upper frame) and Eu (lower frame) including the pure sample ($x = 0$) as

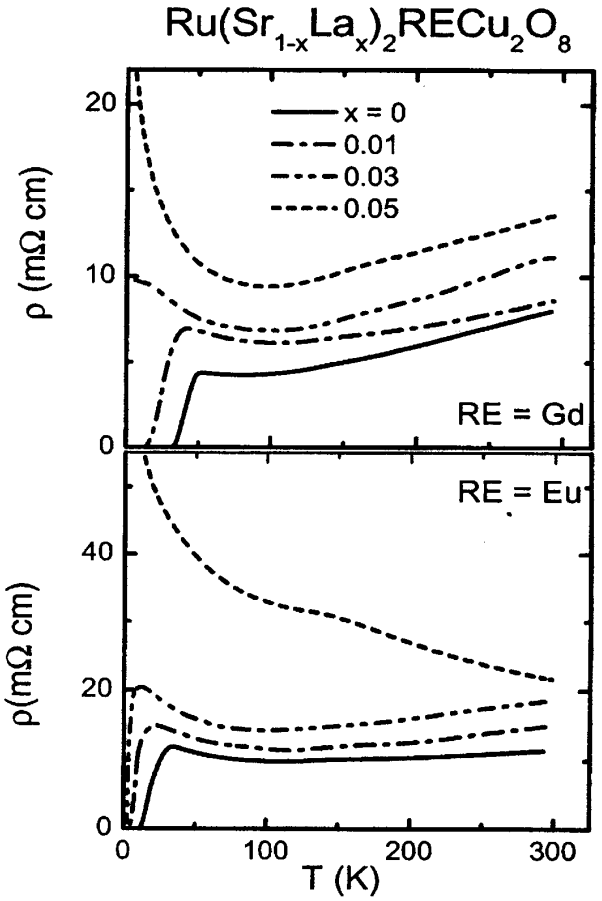

Figure 4. Electrical resistivity versus temperature in zero applied magnetic field for $Ru(Sr_{1-x}La_x)_2RECu_2O_8$ with La concentrations $x = 0$, 0.01, 0.03, and 0.05. Upper frame: RE = Gd, lower frame: RE = Eu.

a reference material. On increasing La-doping, the room temperature resistivity values increase continuously for both rare earth-based compounds. The samples with $x = 0.01$ behave similar to the pure compounds, but the superconducting phase transition T_c is shifted to lower temperatures (by approximately 10 K). For $x = 0.03$ the superconductivity in Ru-1212Gd is fully suppressed whereas Ru-1212Eu is still superconducting below 3 K though the normal state resistivity of the Eu based samples is larger than that of the Gd based samples for the same La concentration x. The resistivity passes through a minimum and reveals a semiconducting temperature characteristic below 100 K with $x > 0.03$. For $x = 0.10$ (not shown in Fig. 4), $\rho(T)$ is strongly enhanced even at room temperature and increases for all temperatures below 300 K. The rapid suppression of superconductivity and the evolution of a semiconducting-like state upon doping by a small amount of La is consistent with the behavior of an underdopedhigh-T_c superconductor. The magnetic phase transition in $Ru(Sr_{1-x}La_x)_2RECu_2O_8$ appears as a weak smeared-out anomaly in the temperature dependent resistivity at around 150 K. This broad anomaly shifts to higher temperatures on increasing x and is confirmed by magnetic measurements [34].

The temperature dependence of the upper critical field H_{c2} contains important parameters that characterize the superconducting state, such as the flux pinning energy and the superconducting condensation energy that are also related to the pairing mechanism. In high-T_c cuprates a remarkable broadening of $\rho(T)$ upon increasing field is observed, mainly due to the flux motion, and hence a large uncertainty arises to define T_c and to determine H_{c2}. Usually, H_{c2} is determined from magnetization measurements. Because of the ferromagnetic ordering of the Ru moments it is difficult to determine H_{c2} from magnetization measurements in Ru-1212RE. In such cases a study of the shift of T_c in the temperature dependence of ρ in magnetic fields is a possible method to determine H_{c2}. To avoid the effect of flux flow, the temperature at which ρ starts to decrease from its normal state value (the maximum value) defined as T_c(max) may be used for the determination of H_{c2}.

The upper frame of Fig. 5 shows $\rho(T)$ of $x = 0.01$ La-doped Ru-1212Gd in different external magnetic fields $0 \leq H \leq 140$ kOe. The superconducting transition temperatures are significantly shifted to lower temperatures but even in the highest field, the sample remains superconducting at low temperatures. Compared to other high-T_c cuprates the resistive broadening is moderate for La-doped Ru-1212Gd and shows no resistive tail at low temperatures. In fact, the transition width ΔT_c between 90% and 10% of the normal-state resistivity is smaller at a magnetic field of 140 kOe than in zero field. The variation of the corresponding upper critical field H_{c2} with temperature as evaluated by using different criteria is shown in the lower frame of Fig. 5. H_{c2} determined from the shift of the transition temperature near the onset of superconductivity (represented in Fig. 5 by solid and open circles, respectively) shows a steep slope with $dH_{c2}/dT \sim 1$ T/K. On the other hand, H_{c2} calculated from the field dependence of $T_c(R = 0)$ exhibits a small slope near T_c but a rapid increase as T approaches 0 K. The absence of a resistive tail and the high value of H_{c2} suggest the presence of strong pinning forces in this system. This indicates that the SC condensation energy due to pairing is large because the pinning energy is proportional to the condensation energy. A similar behavior has also been observed in some other overdoped HTSCs [38, 39]. The temperature dependence of H_{c2} for Ru-1212Gd is qualitatively similar to that observed in $Bi_2Sr_2CuO_6$ (Bi-2201) [40], $La_{2-x}Sr_xCuO_4$ (La-214) [41] and the electron-doped cuprates $Sm_{2-x}Ce_xCuO_{4-y}$ [42,43]. In Bi-2201 and La-214, a second critical transition (T_{c2}) is observed well below T_c^{on} [40]. With increasing magnetic field, T_c^{on} decreases very slowly whereas T_{c2} decreases dramatically and shows a large positive curvature in the critical field.

The thermopower (S) of the pure and all La-doped Ru-1212RE compounds is measured in the temperature range 77 K $\leq T \leq$ 350 K as illustrated in Fig. 6. A systematic evolution of S with temperature and La doping is clearly evident from this figure. At temperatures below 160 K, S shows approximately a linear T- dependence and the slope increases with increasing x. Subsequently, S passes through a broad maximum (at T^s) and decreases on further increasing temperature. With increasing x, the overall magnitude of S increases and T^s shifts towards higher temperatures. Similar results were reported for doped Ru-1212Gd in which Ru was partially substituted by Nb [20]. The large value of S and the shape of $S(T)$ with the appearance of a broad maximum at high temperatures is typical for underdoped high-T_c cuprates.

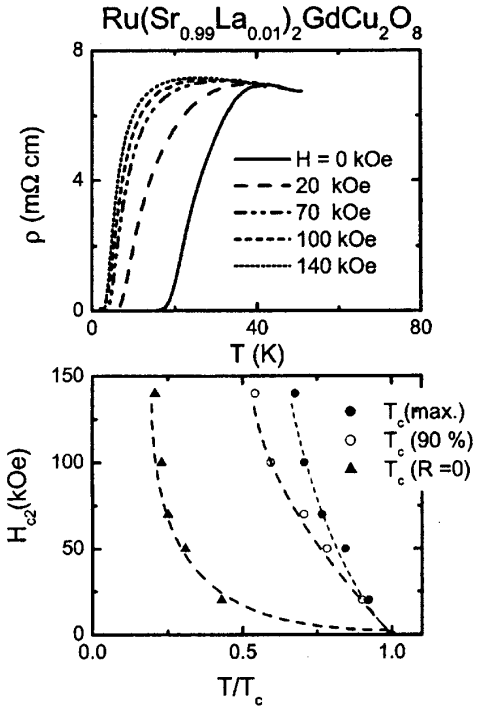

Figure 5. Upper frame: Dc resistivity versus temperature for $x = 0.01$ La-doped Ru-1212Gd in different magnetic fields. Lower frame: The corresponding upper critical field H_{c2}(T) evaluated by using different criteria for determination of T_c. The dashed lines in the lower frame are only to guide the eyes.

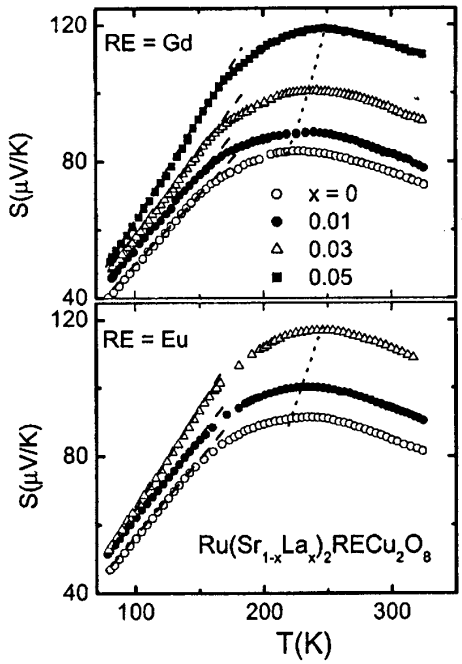

Figure 6. The temperature dependence of the thermoelectric power (S) for pure and La-doped Ru-1212RE compounds, RE = Gd (upper frame) and RE = Eu (lower frame). The dashed lines indicate a linear behavior of S and the dotted curve shows the shift of the maximum with increasing La content for both rare earth based compounds.

In the structurally closely related $YBa_2Cu_3O_{7-\delta}$ (YBCO) system, superconductivity disappears for $\delta > 0.6$. Strikingly, both the magnitude and temperature dependence of S of Ru-1212Gd is comparable to that of YBCO for δ close to 0.6 [44]. In high-T_c cuprates a universal relation between the charge carrier concentration p and the room temperature thermopower $S(T = 300\ K)$ has been established [44]. If we assume that this relationship is also applicable for Ru-1212Gd, then the sample with $x = 0$ corresponds to a hole concentration of $p \approx 0.07$ holes per Cu ion [22]. This indicates a highly underdoped nature of Ru-1212Gd which is consistent with the resistivity behavior. As the substitution of one Sr ion by one La ion corresponds to a reduction of one hole per Cu, the complete suppression of superconductivity at about $x = 0.03$ corresponds to $p = 0.04$/Cu. This value of p is close to the doping level at the border of superconductivity in other cuprates and also close to that predicted by the well-known parabolic relation $T_c/T_{c,max} = 1 - 82.6(p - 0.16)^2$ [19, 45].

The substitution of monovalent Na^+ for Sr^{2+} in Ru-1212Gd is now compared with La-doping. Similar to La-doping, the magnetic ordering temperature is enhanced while below T_M the ferromagnetic component is decreased with increasing Na concentration due to an increase of the canting angle of the Ru moments. A further similar behavior is found in the suppression of superconductivity upon increasing doping concentration of

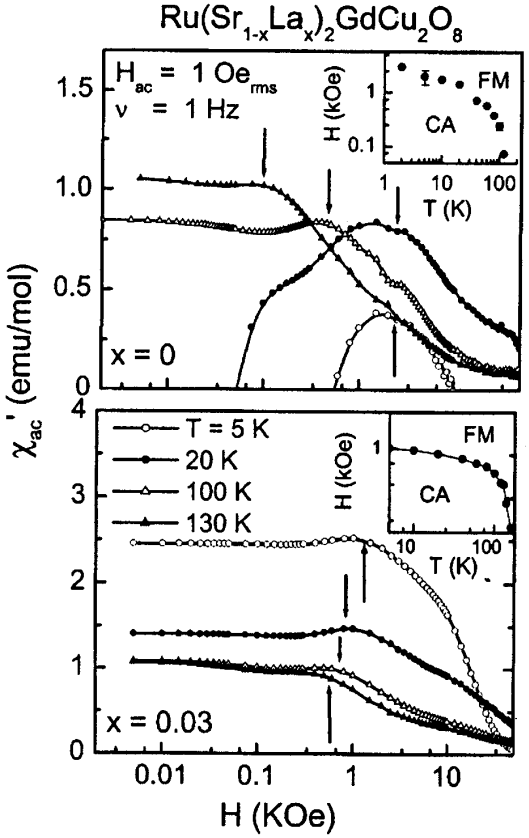

Figure 7. Field dependence of the real part of the ac magnetic susceptibility for the 3% Na doped sample at different temperatures below T_M. The arrows indicate a characteristic temperature where a metamagnetic transition occurs. The inset shows schematically the $H - T$ phase diagram separating a canted antiferromagnetic phase at low fields from a high field ferromagnetic phase.

Na. However, the concentration dependence is slightly different between Na and La doped Ru-1212RE. For a concentration of 3% of Na one clearly observes superconductivity (with an onset transition temperature of T_c = 44 K) whereas 3% La defects completely suppress superconductivity. For 10% of either Na or La, both compounds exhibit very similar physical properties with a semi-conducting like temperature dependence of the resistivity over the entire investigated temperature range. The suppression of superconductivity upon Na doping is unexpected as it corresponds to hole doping in contrast to the electron doping by La substitution. Therefore, the physical mechanism must be different in both substitutional series. Most probable an efficient defect trapping prevents a transfer of charge carriers into the CuO-planes. The field dependence of the real part of the ac magnetic susceptibility for various temperatures is shown in Fig. 7. The data were taken after zero-field cooling at 1Hz with an ac field of 1 Oe from above and below T_M. Maxima in the field dependence of χ can be detected and signal a metamagnetic transition. The corresponding phase diagram, where the solid points separate a ferromagnetic (FM) phase at high fields from a canted antiferromagnetic (CA) phase at low fields is illustrated in the inset of Fig. 7. The $H - T$ phase diagram of the Na doped compounds is similar to the La doped one, where FM phase transition can be induced by fields smaller than 1kOe [34].

6. Phase diagram

Fig. 8 shows the (x, T)-phase diagram for the doped Ru-1212Gd system summarizing some of our pervious results [26, 34]. The superconducting transition temperature was determined as the mid-point of the resistivity decrease towards zero resistance. The magnetic lines are obtained by the fitting of the inverse susceptibility

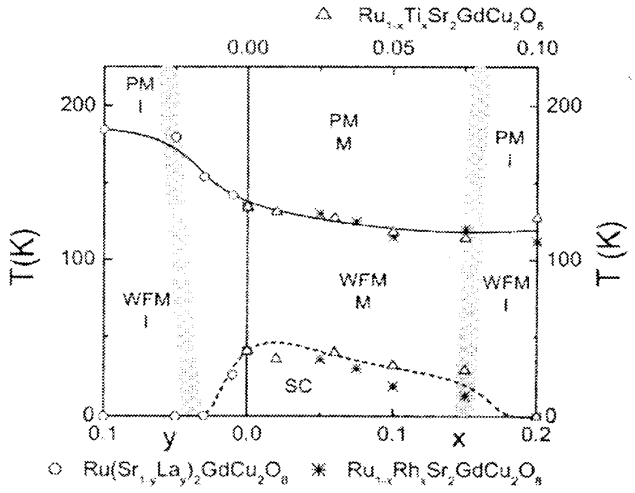

Figure 8. Generalized phase diagram of the Ru-1212Gd system. Plotted is transition temperature vs. doping concentration for different dopants. The doping parameter y (from zero to the left) denotes a decrease of the hole concentration in the system $Ru(Sr_{1-y}La_y)_2GdCu_2O_8$. The doping parameter x corresponds to an increase of the charge carrier density in the systems $Ru_{1-x}M_xSr_2GdCu_2O_8$ with M = Ti (upper scale, $0 \le x \le 0.1$) and Rh (lower scale, $0 \le x \le 0.2$). The shaded areas represent the crossover regions from insulating to metallic behavior as evaluated from $\partial\rho/\partial T$ for temperatures well above T_c.

using two independent Curie-Weiss equations [34]. For La^{3+} doping, superconductivity appears only in a narrow doping range ($x \leq 0.03$), while the magnetic ordering temperature is enhanced with increasing x. On the other hand, substituting Ru by Ti^{4+} ($3d^0$) or Rh^{3+} ($4d^6$) reduces the magnetic ordering temperature of RuO_2 layers but SC survives for a considerable range of doping concentrations ($x \leq 0.075$ for Ti and $x \leq 0.15$ for Rh). It becomes clear from Fig. 8 that 10% Ti suppresses superconductivity, while for the same effect 20% Rh is needed. La^{3+} substitutes Sr^{2+} and reduces the hole concentration in the CuO_2 planes [34]. Rh^{3+} and Ti^{4+} increase hole doping and one would expect that T_c increases. Probably due to disorder and localization effects this is not the fact. However, in case of hole doping superconductivity survives much longer than in case of electron doping. Above T_c up to the magnetic ordering temperature, a weak ferromagnetic metallic (WFM) phase is observed. Close to the critical concentration, where the superconductivity becomes suppressed, a weak ferromagnetic insulator (WFI) shows up. Furthermore, the system is a paramagnetic metal (PM) at temperatures above the magnetic ordering temperatures of the superconducting samples but becomes a paramagnetic insulator (PI) at the critical concentration and low temperatures.

7. Magnetic and non-magnetic doping at the Cu site: Co, Ni, Ga, Zn

The upper frame of Fig. 9 shows the effect of Ga impurities (upper frame) on Ru-1212Gd as a typical example of copper substitution. The resistivity increases with increasing Ga concentration and the superconductivity was fully suppressed at $x = 0.03$ (as shown in the lower frame of Fig. 9). The lower frame of the figure shows the normalized resistivity for $RuSr_2Gd(Cu_{1-x}A_x)O_8$ at a concentration $x = 0.03$ for A=Ga, Ni, Co, Mn. All these samples are non-superconducting and the resistivity shows a semiconductor-like behavior similar to that observed for other Cu substituted high-T_c superconductors. The change of T_c for different cations is summarized in the inset of Fig. 9. Both Mn and Co suppress the superconductivity faster than Ga or Ni. This may be attributed to their large magnetic moment which may lead to a stronger pair breaking effect. However, Hodges *et al.* [46] reported that the disorder induced by the presence of Co at the copper site in YBCO leads to the simultaneous coexistence of a superconducting and a magnetic order parameter without any detrimental interference. The coexistence of superconductivity and antiferromagnetism (AFM) of YBCO was described as an inhomogeneous state associated with the formation of granular AFM phases within a d-wave superconductor. Moreover, the superconductivity in YBCO is in general not rapidly suppressed by the substitution of other 3d elements at the Cu site [47–50]. It is observed that T_c is reduced to zero beyond a critical concentration which varies from element to element. In some cases, superconductivity is preserved for a large concentration range reaching maximal values of $x = 0.30$ for Fe or Co and $x = 0.50$ for Ni doping, respectively.

Tallon *et al.* [22] and Bernhard *et al.* [51] studied the substitution of Zn at the Cu site in Ru-1212Gd and observed that superconductivity is completely suppressed at a concentration of 3% Zn while the magnetic susceptibility is enhanced at low temperatures. This behavior is attributed to pair breaking. The extreme sensitivity of superconductivity towards Zn doping is well known from other high-T_c materials and has been studied in detail for $YBa_2Cu_3O_{7-\delta}$(YBCO) and $La_{x-2}Sr_xCuO_{4-\delta}$(LSCO) systems [52, 53].

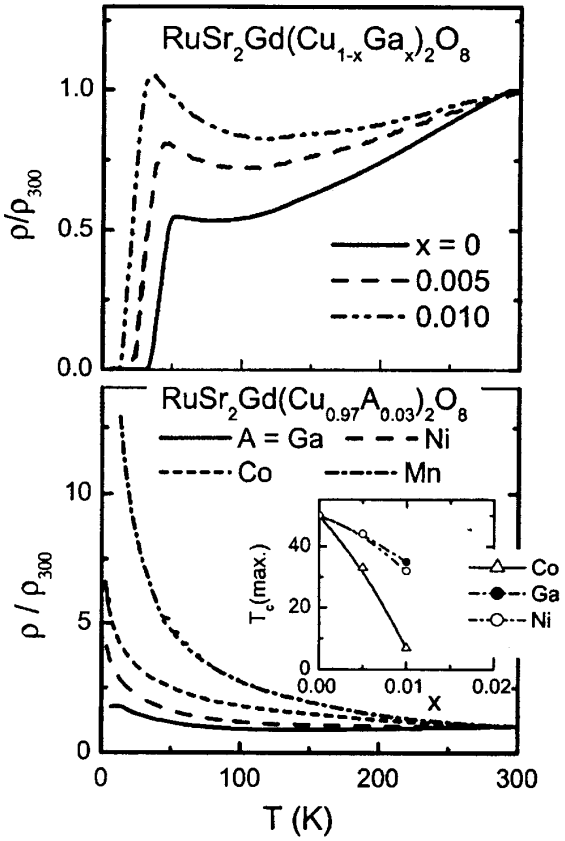

Figure 9. Normalized electrical resistivity versus temperature for Ga-doped Ru-1212RE (upper frame). The lower frame shows the normalized resistivity of all non-superconducting samples of $RuSr_2Gd(Cu_{0.97}A_{0.03})O_8$, where A = Ga, Ni, Co and Mn. The inset displays the dependence of T_c versus concentration x for some different cations.

In Fig. 10, the resistivity of the Zn-doped Ru-1212Eu samples are compared to Zn-doped Ru-1212Gd [22]. For Zn-doped Ru-1212Eu, the samples exhibit a small change of the slope around the magnetic ordering temperature while in Zn-doped Ru-1212Gd no clear change in the resistivity is observed around T_M.

8. Conclusions

We gave a detailed account on the optimized sample preparation conditions. Furthermore, we have successfully synthesized two novel substitutional series $Ru(Sr_{1-x}Na_x)_2GdCu_2O_8$ ($0 \leq x \leq 0.10$) and $RuSr_2Gd(Cu_{1-x}M_x)_2O_8$ (M = Co; Ni; Ga; $0 \leq x \leq 0.03$). Powder x-ray diffraction revealed single phase materials and only minor crystallographic changes as compared to pure Ru-1212Gd for all investigated compounds. Changes of the physical behavior of Ru-1212Gd are known to be sensitive to both, substituent and substitutional site. Na doping has been chosen in order to study the effect of hole doping and the substitution of Sr by La for studying electron doping at the Sr site. Similar to the effect of La-doping, T_M is enhanced and T_c suppressed by Na-doping but at a different rate. As monovalent Na-doping increases the hole concentration in the system because it substitutes a divalent cation (Sr^{2+}) the decrease of T_c with increasing Na concentration must be attributed to other effects like trapping of charge

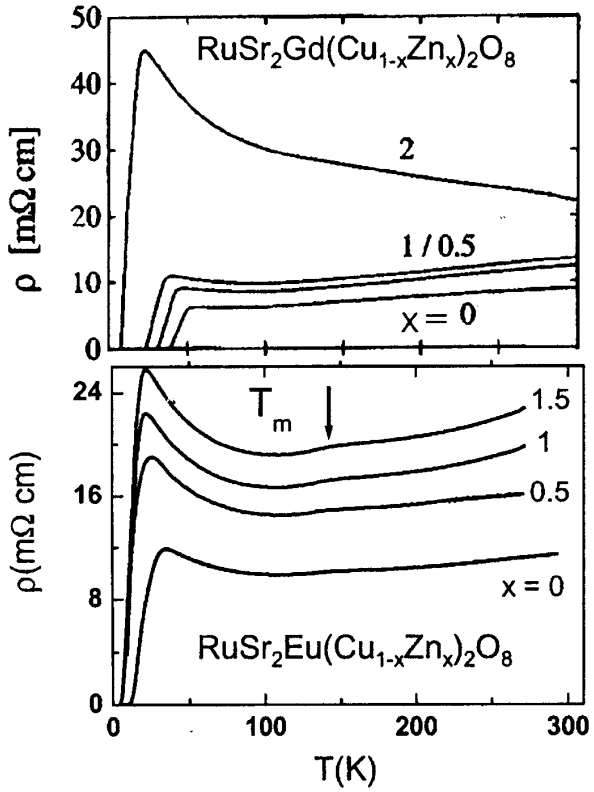

Figure 10. Upper frame: Temperature dependence of the resistivity of Zn doped Ru-1212Gd. The numbers indicate the Zn concentration in %. (taken from Ref. [22]). Lower frame: The dc resistivity versus temperature of Zn-doped Ru-1212Eu (again concentrations are given in %) .

carriers. Moreover, exchange of Cu ions for Co, Ni or Ga respectively probes the effect of impurities within the superconducting CuO-planes. Superconductivity is suppressed rapidly by copper substitution due to pair-breaking as generally observed in high-T_c superconductors. The effect of Co substitution is stronger than the effect of magnetic Ni or non-magnetic Ga impurities because of its large magnetic moment. Compared with 3*d*-element doped YBCO, superconductivity is destroyed very rapidly in Ru-1212RE. This implies that the major contribution to superconductivity originates from the copper-oxide planes. The decrease of the magnetic moment at low temperatures for Ga substitution and its increase for Co or Ni suggests that there is a contribution of the CuO-planes to the total magnetic moment of the system.

9. Acknowledgments

This work was partly supported by Bundesminterium für Bildung und Forschung (BMBF) via VDI/EKM 13 N 6917 and by the Deutsche Forschungsgemeinschaft via SFB484, Augsburg.

References

1. V. L. Ginzburg, Sov. Phys. JETP, **4**, 153 (1957).
2. "Superconductivity in ternary compounds", edited by M. B. Maple and Ø. Fisher, (Berlin, **II**,1982).

3. L. N. Bulaevskii et al., Adv. Phys. **34**, 176 (1985).
4. P. Fulde and R. A. Ferrell, Phys. Rev. **135**, A550 (1964); A. I. Larkin and Yu N. Ovchinnikov, Zh. Eksp. teor. Fiz **47**, 1136 (1964).
5. L. Bauerfeind, W. Widder and H. F. Braun, Physica C 254, 151 (1995); J. Low Temp. Phys. **105**, 1605 (1996).
6. I. Felner et al., Physica C **311**, 163 (1999).
7. C. Artini et al., Physica C **377**, 431 (2002).
8. T. Papageorgiou et al., Physica C in press.
9. J. W. Lynn et al., Phys. Rev. B **61**, 14964 (2000).
10. J. D. Jorgensen et al., Phys. Rev. B **63**, 54440 (2001).
11. G. V. M. Williams and S. Krämer, Phys. Rev. B **62**, 4132 (2000).
12. J. Hemberger et al., Phys. Rev. B **66**, 094410 (2002).
13. R. S. Liu et al., Phys. Rev. B **63**, 212507 (2001).
14. H. Aliaga and A. A. Aligia, Physica B **320**, 34 (2002).
15. K. Kumagai, S. Takada and Y. Furukawa, Phys. Rev. B **63**, 180509 (2001).
16. K. Otzschi et al., J. Low. Temp. Phys, **117**, 855 (1999).
17. P. W. Klamut et al., Physica C **341-348**, 455 (2000).
18. B. Lorenz et al., Physica C **363**, 251 (2001).
19. J. Tallon et al., IEEE. Trans. App. Super, **9**, 1696 (1999).
20. A. C. McLaughlin and J.P.Attfield, Phys. Rev. B **60**, 14605 (1999); A.C. McLaughlin et al., J. Mater. Chem. **11**, 173 (2001).
21. M. Hrovat et al., J. Mater. Sci. Lett., **19**, 919 (2000); M. Hrovat et al., J. Mater. Sci. Lett., **19**, 1423 (2000).
22. J. L. Tallon et al., Phys. Rev. B **61**, 4671 (2000).
23. J. L. Tallon et al., J. Low Temp. Phys. **117**, 823 (1999).
24. L. Bauerfeind, Ph. D. thesis, University of Bayreuth, (1998).
25. P. W. Klamut et al., Physica C **350**, 24 (2001).
26. A. Hassen et al., Physica C, accepted for publication (2003).
27. J. Rodriguez-Carvajal, Physica B **192**, 55 (1993).
28. J. B. Mandal et al., Phys. Rev. B **46**, 11840 (1992).
29. O. Chmaissem et al., Phys. Rev. B **61**, 6401 (2000).
30. K. L. Nakamura et al., Phys. Rev. B **63**, 024507 (2000).
31. G. M. Kurz'micheva et al., Physica C **350**, 105 (2001).
32. A. C. McLaughlin et al., Phys. Rev. B **60**,7512 (1999).
33. V. P. S. Awana et al., J. Appl. Phys. **91**, 8501 (2002).
34. P. Mandal et al., Phys. Rev. B **64**, 144506 (2002).
35. P. W. Klamut et al., Phys. Rev. B **63**, 224512 (2001).
36. J. T. Rijssenbeek et al., Physica C **341-348**, 481 (2000).
37. S. Malo et al., J. Inorg. Mater. **2**, 601 (2000).
38. A. P. Mackenzie et al., Phys. Rev. Lett. **71**, 1238 (1993).
39. M. S. Osofsky et al., Phys. Rev. Lett. **71**, 2315 (1993).
40. H. H. Wen et al., Phys. Rev. Lett. **85**, 2805 (2000).
41. H. H. Wen et al., Phys. Rev. Lett. **82**, 410 (1999).
42. Y. Dalichaouch et al., Phys. Rev. Lett. **64**, 599 (1990).
43. Y. Hidaka and M. Suzuki, Nature (London) **338**, 635 (1989).
44. S. D. Obertelli et al., Phys. Rev. B **46**, 14928 (1992).
45. M. R. Presland et al., Physica C **387**, 95 (1991).
46. J. A. Hodges et al., Phys. Rev. B **66**, 020501 (2002).
47. J. M. Tarascon et al., Phys. Rev. B **36**, 8393 (1987).
48. J. M. Tarascon et al., Phys. Rev. B **37**, 7458 (1987).
49. G. Xiao et al., Phys. Rev. B **35**, 8782 (1987).

50. D. M. Ginsberg, Physical Properties of High Temperature Superconductors I, World Scientific, Singapore (1989).
51. C. Bernhard et al., Phys. Rev. B **59**, 14099 (1999).
52. B. Nachumi et al., Phys. Rev. Lett. **77**, 5421 (1996).
53. Y. Fukuzumi et al., Phys. Rev. Lett. **76**, 684 (1996).